

Cation-Type Dependences of ^1H and ^{29}Si MAS NMR Chemical Shifts and Desorption Temperatures of Water Molecules in Faujasite-Type Zeolites

Tomohiro Morita¹, Hisashi Honda^{1,2,3*}, Tatsuto Katayama²,
Susumu Tanaka⁴ and Shin'ichi Ishimaru⁵

¹International Graduate School of Arts and Sciences, Yokohama City University,
Kanazawa-ku, Yokohama, 236-0027, Japan.

²International College of Arts and Sciences, Yokohama City University, Kanazawa-ku,
Yokohama, 236-0027, Japan.

³Graduate School of Nanobioscience, Yokohama City University, Kanazawa-ku, Yokohama,
236-0027, Japan.

⁴Department of Materials Science, Yonago National College of Technology, Yonago, 683-
8502, Japan.

⁵Department of Green and Sustainable Chemistry, Tokyo Denki University, Chiyoda-ku,
Tokyo, 101-8457, Japan.

Authors' contributions

This work was carried out in collaboration between all authors. All authors contributed in practical work and managed the analysis of the study. All authors read and approved the final manuscript.

Original Research Article

Received 19th March 2014

Accepted 28th May 2014

Published 20th June 2014

ABSTRACT

In order to reveal adsorbed states of water molecules on faujasite-type zeolites (FAU) systematically, twenty five kinds of FAU were prepared in this study: Na ions in FAU with Si/Al ratios of 1.0, 1.2, 1.7, 2.4, and 3.5 were exchanged by each Li, K, Rb, and Cs ions. High-resolution solid-state ^1H NMR spectra with a magic-angle-spinning (MAS) method showed a signal which can be assigned to H atoms of water molecules adsorbed on each FAU. Complex dependences of ^1H chemical-shift (CS) value on cation types were

*Corresponding author: Email: hhonda@yokohama.cu.ac.jp;

recorded (the lowest CS value was detected in Na- or K-type FAU with each Si/Al ratio). The similar tendency was recorded on ^{29}Si MAS NMR spectra. In addition, thermogravimetry (TG) and differential-thermal-analysis (DTA) lines showed that a desorption temperature of water molecules was increased with decreasing Si/Al ratios, conversely, the temperature showed complex dependences on cation properties (the minimum temperature was recorded in Na- or K-type FAU with each Si/Al ratio). In our simulations, the similar complex relations recorded on the ^1H and ^{29}Si MAS NMR spectra were obtained by use of a supercage model.

Keywords: Faujasite; water; adsorption; solid-state ^1H NMR.

1. INTRODUCTION

Zeolites are microporous crystalline materials and constructed by SiO_4 and AlO_4 units. Zeolite's types are classified by crystalline structures and Si and Al ratios (Si/Al). Faujasite-type zeolites (FAU) are one of the zeolites, widely used in chemical industries and scientific endeavors, because of their special structure and properties of adsorption, ion exchange, and catalysis [1-7]. The general chemical formula of FAU in an unit cell is $M_{(x/n)}(\text{SiO}_2)_{(192-x)}(\text{AlO}_2)_x \cdot y\text{H}_2\text{O}$, where M is a cation of charge $+n$. The number x of cations can vary from 0 to 96, depending on the Si/Al ratio. The number of water molecules (y) in the unit cell is depended on steam pressure. The crystalline structure of FAU as well as the position of the M cations is determined by X-ray and neutron diffraction measurements [8,9]. The unit framework of FAU is constructed by sodalite cages combined by hexagonal prisms each other, and makes a pore (it is called as supercage). The substitution of Si with Al atoms in the FAU framework induces a net negative charge on the framework. To keep the overall framework to the neutral charge, the M ions are distributed at three kinds of specific position in FAU: Sites I (SI) are located in the center of hexagonal prism, while the sites I' (SI') are present in the sodalite cage toward the hexagonal prism, sites II (SII) is located in the six-ring windows, and sites III (SIII) and III' (SIII') are located in the center of the four-ring and twelve-ring windows of the supercages, respectively [10,11]. It is also known that cations occupy whole SI, SI', and SII in FAU with any Si/Al ratio, in contrast, population of SIII and SIII' is increased with decreasing Si/Al ratios in a range of Si/Al ratio < 2 [9-11]. The cation at SII, SIII, and SIII' can be immediately exchanged by other cations in solutions. It is reported that the size and valence of the M ion are critically important in adsorption capacities and catalytic properties [6]. FAU with low Si/Al ratios shows hydrophilic characters because the M ions attract water molecules by strong electrostatic interactions. Therefore, the presence of water molecules in FAU cannot be avoided in many applications, especially, operating at ambient temperature. Molecular dynamics (MD) and molecular orbital (MO) simulations show informations of the water molecules and the cation sites in FAUs [10-18]. MD simulations show a three-step mechanism of water adsorption on FAU: water molecules are firstly adsorbed around the M ions in FAU, the next water molecules form a monolayer on the FAU surface, and the further waters (the third step) are located in the supercage [12]. In addition, another MD calculation reports that the first water molecules are adsorbed on the cations located at SI (SI') and SII in FAU with $\text{Si/Al} > 2$, in contrast, in a case of small Si/Al ratios, the water molecules interact with cations at the whole sites of cations [13,14]. Based on these reports, the cations can locate at SIII and SIII' and interact with water molecules in only $\text{Si/Al} < 2$. Grand-Canonical-Monte-Carlo (GCMC) demonstrations explain Si/Al ratio dependences on adsorption isotherms and heats observed in Na-type FAU [10,11,15,16]. These simulations are generally performed for the unit cell model of hydrated and

anhydrated FAUs. In a case of MO simulations, small cluster models, which are local parts of the FAU framework, have been frequently used [17-23]. Second-order Moller-Plesset (MP2) and density-functional-theory (DFT) methods show good agreement with the experimental proton-affinities (PA) values, although small cluster models of $(\text{H}_3\text{SiO})_4\text{AlH}$ and $\text{AlSi}_{10}\text{O}_{14}\text{H}_{17}$ (three four-rings and one six-ring are combined) are employed [17]. In a case of ^{29}Si NMR methods, it is reported that Si-O-Si angles in zeolite frameworks strongly contribute to ^{29}Si chemical shift (CS) values [20-23]. Experimental studies also report that the location of these M ions plays a crucial role on the thermodynamics, molecular dynamics, catalysis, and adsorbents in FAUs. The interactions between water molecules and FAUs have been revealed by adsorption and desorption isotherms, infra-red (IR), Raman, diffuse reflectance infrared Fourier transform spectroscopy (DRIFTS), NMR, and dielectric measurements, etc. [1-8,24-36]. DRIFTS spectra reveal the formation of strongly bonded water-cation clusters in zeolites [24]. IR and Raman spectra show that bending vibrations of FAU framework are linked with the unit-cell sizes and the vibrations are influenced by the charge distribution within FAU [25]. Solid-state ^{29}Si , ^{27}Al , and ^1H NMR measurements of FAU are performed with a magic-angle-spinning (MAS) method to determine Si/Al ratios and to study acid sites of FAU [27-32]. However, ^1H MAS NMR spectra with high speed MAS (>30 kHz) are rarely reported as functions of Si/Al ratios and cation types in hydrated FAU. In this study, TG-DTA, N_2 adsorption isotherms, and ^1H and ^{29}Si MAS NMR measurements were performed in twenty five kinds of FAU with Si/Al ratios of 1.0, 1.3, 1.7, 2.4, and 3.5, in addition, and with cations of Li, Na, K, Rb, and Cs, in order to reveal water molecules states in FAUs.

2. MATERIALS AND METHODS

2.1 Sample Preparation

In this study, two commercial FAUs of Na form (Tosoh Co.) with Si/Al ratio of 1.2 and 2.4, and three specimens (abbreviated to Sample A, B, C) prepared by modifying a recipe of the previous report [37], were employed. Sample A, B, and C were synthesized by the following process.

2.1.1 Sample A

Sodium aluminate (5.59g), potassium hydroxide (5.38g), sodium hydroxide (7.77g), and sodium silicate (11.50g) were dissolved in aqueous solution (85.90g) and mixed thoroughly. Obtained aqueous solution was incubated at 342K for 14 hours and agitated at 368 K for 4 hours in vessel sealed with Teflon. After filtering, obtained specimens were washed by a 0.01 M sodium hydroxide solution and dried at room temperature.

2.1.2 Sample B

Sodium hydroxide (1.48g) and sodium aluminate (0.76g) were poured in water (7.17g) and stirred until completely dissolved. Sodium silicate solution of 27.3% (39.21g) was added into the solution and stirred at room temperature for 1 day. Another concentration of sodium hydroxide (0.1%), sodium aluminate (9.1%) and sodium silicate (37.6%) aqueous solution of 92.66 g was transferred into the prepared solution and let the mixed solution for 1 day after stirring for 30 minutes. After incubation of 7 hours at 373 K, obtained samples were washed by water and dried at room temperature.

2.1.3 Sample C

Sodium hydroxide (1.65g) and sodium aluminate (3.64g) were added into 15-crown-5 ether (2.25g) of aqueous solution (17.75g). Silica sol (Nissan Chemical Industries, Ltd. Snotecs 40) of 30.0g was dissolved in the solution. This solution was stirred with a magnetic bar at approximately 200rpm for 1 day at room temperature. Zeolite crystals were obtained by keeping it in Teflon-lined stainless steel autoclave at 383K for 10 days. After washing with water until pH of the filtrate solution achieved to 6, crystals were dried at room temperature overnight. In order to remove template of 15-crown-5 ether from the crystal, temperature of the sample was increased with 3K min^{-1} until 423K and kept the same temperature for 1 hour. After this manipulation, the sample was successfully heated with 3K min^{-1} until 643K and kept at the temperature for 3 hours. Oxygen gas was run into the oven with flow speed of 150ml min^{-1} for the calcination. All sample preparation described above were carried out by employing an AdvantecFS-605 electric drying oven with Isuzu auto tuning control system and an autoclave of 302AC-T304-101503 (Parr Instrument Company Moline).

2.1.4 Ion exchange

Ion exchanged FAUs were prepared by the following manipulation: Na-type FAU added into 1M MCl aqueous solution (M=Li, K, Rb, Cs) and the solution was stirred at ca. 340K by 24 hours. After filtering of ion-exchanged specimens from the solution, M-type FAU was washed by water and dried at room temperature.²³Na MAS NMR measurements observed at a Larmor frequency of 158.75MHz with the MAS speed of 10kHz showed ion-exchanged ratios of 100% (Li), 100% (Na), 100% (K), 60% (Rb), and 60% (Cs), where these values have error within $\pm 5\%$. The low ratios recorded in Rb- and Cs-type FAU can be explained by six-ring window-size of FAU frameworks: Since Rb^+ (296pm) and Cs^+ (338pm) have large ion-size competing with the window-size of ca. 250pm, Na^+ ions located in sodalite cages can't be exchanged.

In this literature, M-type FAU with Si/Al ratio of x is abbreviated to Mx; e.g. K2.4 means K-type FAU with Si/Al=2.4.

2.2 Measurement

^1H and ^{29}Si MAS NMR measurements were carried out by using a Bruker Avance 600 spectrometer (14.10T) with MAS accessory. Solid-state high-resolution ^1H MAS NMR spectra were recorded at a Larmor frequency of 600.13MHz with a MAS speed of 30kHz. Powdered FAU samples and a small amount of silicon rubber were packed in a ZrO_2 rotor with an outer diameter of 2.5mm. Here, silicon rubber is aim to be inner reference of ^1H chemical shifts ($\delta=0.12\text{ppm}$). Si/Al ratios were determined by observing ^{29}Si MAS NMR spectra at 119.22MHz with a MAS ratio of 10kHz. Powdered samples and silicon rubber were packed into a ZrO_2 rotor with an outer diameter of 4.0mm. Here, silicon rubber is inner reference of ^{29}Si chemical shifts ($\delta=-22.59\text{ppm}$). All spectra of ^1H and ^{29}Si nucleus were obtained from free-induction-decay signals which were recorded after a $\pi/2$ pulse. A pulse sequence of ^{29}Si MAS NMR was designed with a ^1H decoupling pulse. Recycle times of 5 and 60 s were employed on ^1H and ^{29}Si MAS NMR measurements, respectively.

In order to confirm that crystal structures of prepared specimens constructs to FAU networks, powder X-ray diffraction (XRD) patterns were measured by a Rigaku RINT 2100 and a

Bruker D8 ADVANCE diffractometer in a scan range of 5 and 50° in steps of 0.02° with a Cu anticathode.

TG, differential TG (DTG) and DTA curves were recorded from 293 to 673 K at heating rate of 5K min⁻¹ with a Seiko Instrument Inc. TG/DTA 6300 apparatus, where Al₂O₃ powder was used for standard sample.

N₂ adsorption isotherms were observed at 77K by using a Bell Japan Inc. BELSORP-mini II. Before the adsorption experiments, all samples were crushed in a mortar and were heated at 673K for 5 hours in vacuum.

2.3 Simulation

Computer calculations were carried out by using a Gaussian 03 program to estimate locations of water molecules, alkali-metal ions, and terminal H atoms in the FAU framework and to simulate shielding tensors of ¹H nucleus in water molecules. Since alkali-metal ions (especially Cs ion) take with many electrons, therefore, a B3LYP/LanL2DZ function was employed for optimization of water molecules and alkali-metal ions in the FAU framework. Shielding tensor estimation of ¹H nucleus was performed by an ONIOM (MP2/cc-pVDZ: HF/cep-4G) method; where shielding tensor of water molecules were estimated by the MP2/cc-pVDZ function, and the other atoms in the frameworks were done by using HF/cep-4G. In the case of ²⁹Si nucleus, shielding tensors were calculated by the B3LYP/LanL2DZ function in another framework model.

3. RESULTS AND DISCUSSION

3.1 XRD and ²⁹Si MAS NMR Measurements

XRD spectra recorded in commercial and prepared FAUs are shown in Fig. 1. The powder patterns reveal that all characteristic FAU peaks are closely match with those reported in the previous report [38] and Sample C retains the FAU structure after the calcination. The result that the similar patterns were obtained in whole FAUs suggests that lattice constants of the FAUs are independent by cation exchanges.

²⁹Si MAS NMR spectra observed in FAUs are displayed in Fig. 2. These lines were able to be analyzed by several Gaussian functions (Lorentz functions could not be fitted well). Substituting each area obtained by fitting the Gaussian function into the following relation [27], Si/Al ratio of 1.0, 1.7 and 3.5 were obtained for Sample A, B and C, respectively, and 1.2 and 2.4 for commercial specimens. These Si/Al values could be estimated within ±0.05.

$$\text{Si/Al} = \frac{\sum A_n}{\sum 0.25nA_n} \quad (1)$$

Here, n and A_n denote the number of Al atoms bonding to a SiO₄ unit and an area of each analyzed curve, respectively. The similar line-shapes were recorded on the ²⁹Si MAS NMR spectra of the same Si/Al ratio (it is the same meaning of independent on cation types). This result suggests that the Si/Al ratio is rarely changed on cation substitutions. In contrast, complex dependences of chemical shift (CS) values on cation types were obtained: the lowest CS values were observed in K- or Rb-type FAU in the same Si/Al ratio. In reported MO simulations [21,22], it is shown that ²⁹Si CS values are decreased with increasing angles

of Si-O-Si in the zeolite framework. In contrast, our XRD spectra were rarely changed with Si/Al ratios and cation types, therefore, it can be considered that Si-O-Si angles in the FAU framework were retained by ion exchanges. In order to reveal the complex dependences recorded on the ^{29}Si MAS NMR spectra, we performed MO simulations. Results are described in section 3.5.

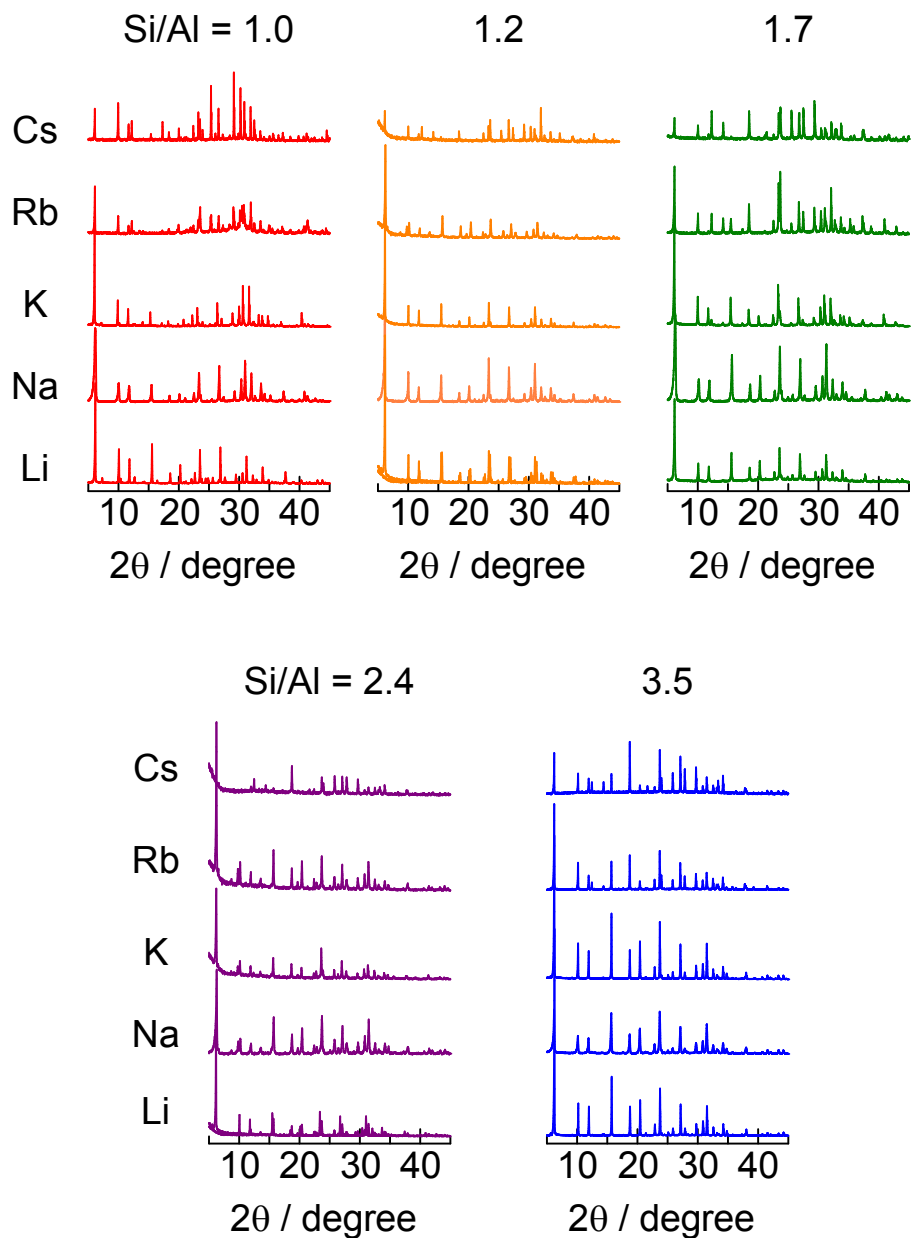


Fig. 1. XRD spectra of M-type faujasite zeolites (M = Li, Na, K, Rb, Cs) with Si/Al ratios of 1.0, 1.2, 1.7, 2.4 and 3.5

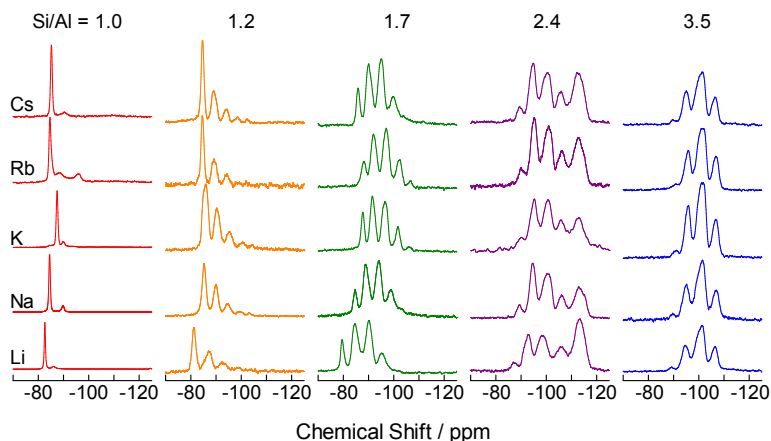


Fig. 2. Influences of Si/Al ratios on ^{29}Si MAS NMR spectra of M-type faujasite zeolites (M = Li, Na, K, Rb, Cs)

3.2 N_2 Adsorption Isotherm Measurements

In order to reveal removing conditions of the water molecules from FAUs, N_2 adsorption isotherms measurements were observed as a function of desorption times. N_2 adsorption isotherms measurements of Na1.0 were carried out after degas handling at 673 K in vacuum for 5, 10, and 15 hours, because FAU with Si/Al ratio of 1.0 is the highest hydrophilicity in the FAUs treated on the present study. Results of N_2 adsorption isothermal measurements are shown in Fig. 3. Slops at low relative pressures in these curves are linked to micropore capacities. Since whole adsorption curves at low relative pressures showed the similar tendencies as displayed in Fig. 3, the pre-observation condition of 5 hours at 673K in vacuum were employed for all N_2 adsorption isotherm measurements in this study (Since we interested in micropore characters of FAUs, the different values recorded at high relative pressure are not important in this study).

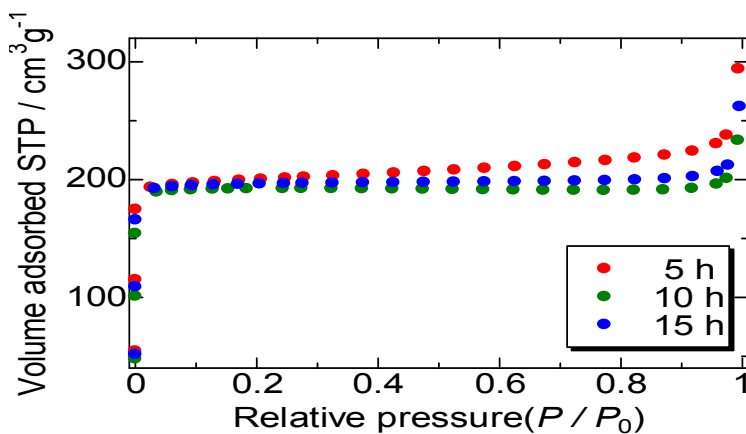


Fig. 3. N_2 adsorption isotherms of Na-type faujasite zeolites with the Si/Al ratio of 1.0 (Na1.0) after water molecules removed from the zeolites at 673 K for 5 h (●), 10 h (●) and 15 h (●)

The result of N₂ adsorption isotherms in each FAU are shown in Fig. 4. These figures reveal that whole FAUs manipulated in this study take the I-type adsorption curve of the IUPAC classification: N₂ molecules adsorb in micro and macro pores of FAUs in the range of low and high relative pressures, respectively. The isotherm curves also show small amount of N₂ molecules adsorbing on Rb- and Cs-type FAUs comparing with those of the other types, as displayed in Fig. 4, although the similar lattice constants were recorded by our XRD measurements. These dependences are similar to reported tendencies [38]. Pore size distribution curves can be generally obtained by N₂ adsorption isotherm measurements, however, low resolution spectra were obtained. Therefore, only tendencies can be discussed for pore sizes in this study. These N₂ adsorption results can be considered that the majority of a large ion is shared in a part of the super cage space: ca. 250pm of windows size of six-ring is smaller than 296 (Rb⁺) and 338pm (Cs⁺) in diameter, and similar to 266pm (K⁺), and larger than 120 (Li⁺) and 190pm (Na⁺) [39]. Other discussions are described in section 3.5.

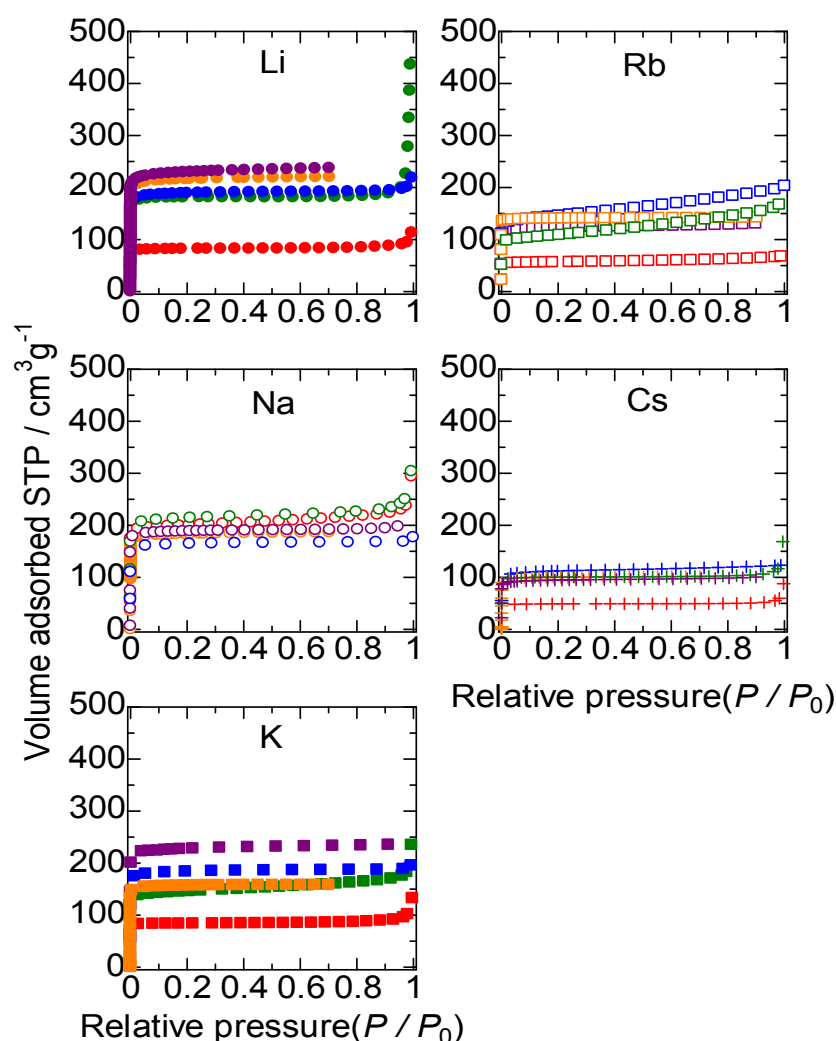
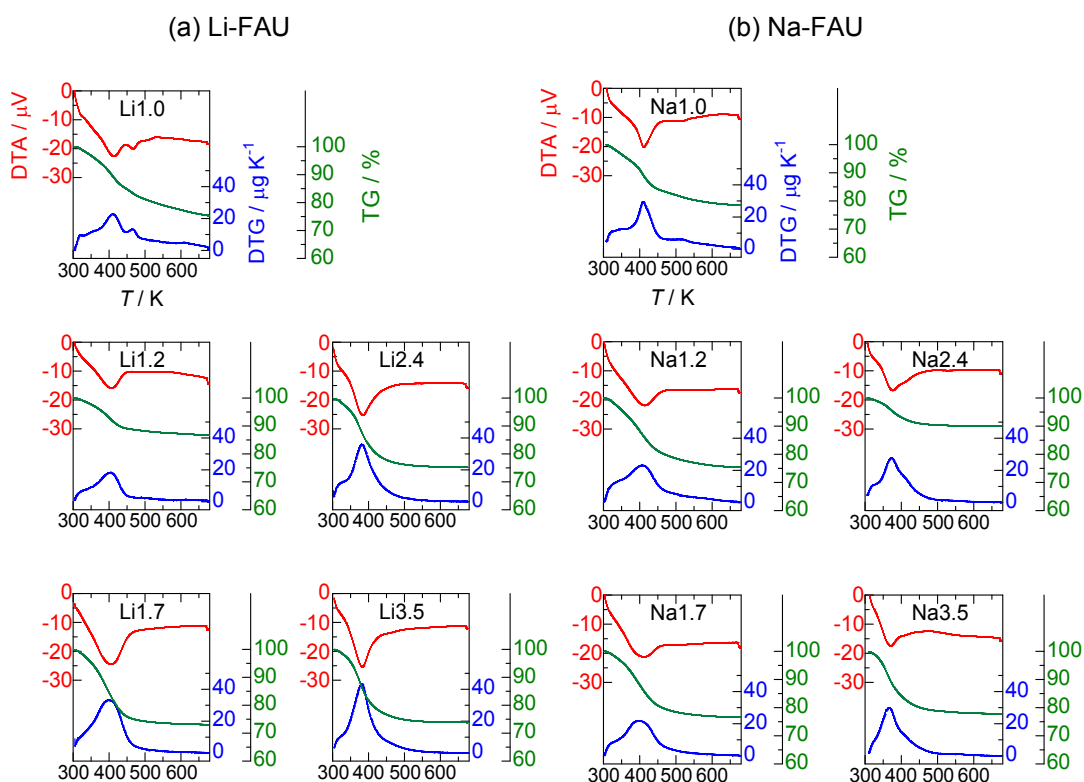


Fig. 4. N₂ adsorption isotherms of faujasite zeolites as a function of Si/Al ratios of 1.0 (red), 1.2 (orange), 1.7 (green), 2.4 (purple) and 3.5 (blue)

3.3 TG/DTA Measurements

DTA, TG, and DTG curves obtained in each FAU are shown in Fig. 5. The endothermic peak were observed at around 400 K. Since weight loss was also recorded at the temperature, this endothermic signal can be attributed to water desorption from each FAU. The origin of the broad signal of DTA and successive decreasing of TG curves can be considered that there are some states of water molecules in FAU: some ones interact with FAU frameworks, others are affected by cation, and the others are located around the center of supercage in FAU [12]. Since it is difficult to determine desorption temperature of water molecules uniquely, a temperature with the largest slope on TG curves (T_{DTG}) was introduced. Here, T_{DTG} is a peak temperature of each DTG curve and means a temperature at which abundant water molecules are removed from FAU. Each T_{DTG} value estimated is listed in Table 1. Based on these values, the higher T_{DTG} is obtained in the lower Si/Al ratios. Since it is well known that cations in zeolites attract water molecules by strong electrostatic interactions, this tendency can be explained by hydrophilicity of FAU (the lower Si/Al ratio results in the higher concentration of cations in FAU). It means that the T_{DTG} value links to a factor of strength of hydrogen bonding among water molecules and cations in FAU. In the case of cation-type dependencies, complex tendencies were recorded: The smallest T_{DTG} was obtained in K- or Na-type FAU as shown in Table 1. This tendency is similar to those observed in the ^{29}Si NMR CS values. Detail discussion about this tendency is described in section 3.5.



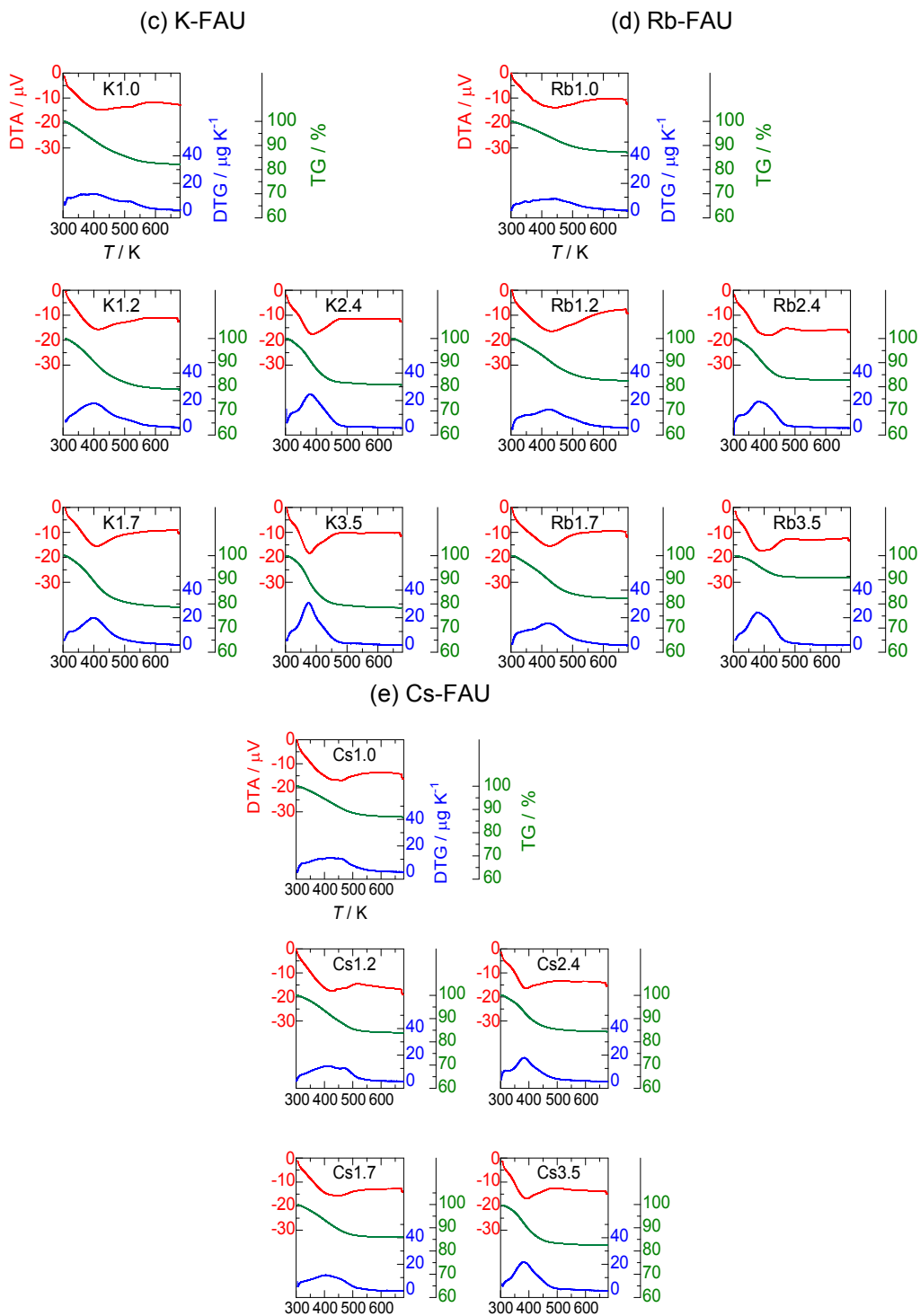


Fig. 5. DTA, TG, and DTG curves observed in M-type faujasite zeolites as a function of temperatures. M = (a)Li, (b)Na, (c)K, (d)Rb, (e)Cs

Table 1. Temperatures with the largest slope on each TG curve (T_{DTG}) of hydrated FAU. Unit is in K. Errors of temperatures are within 1 K, in the case of K1.0, Rb1.0, Cs1.0, and Cs1.7, those are within 3 K

Si/Al Ratio	Li	Na	K	Rb	Cs
1.0	411	408	398	443	419
1.2	405	406	397	418	413
1.7	400	398	397	423	403
2.4	380	371	378	381	384
3.5	380	366	374	375	383

3.4 ^1H MAS NMR Chemical Shift

^1H MAS NMR spectra observed with a MAS ratio of 30kHz are shown in Fig. 6. Two Lorentz-type signals were recorded on each spectrum. Peaks observed at 0.12ppm and around 5ppm can be assigned to H atoms in silicon rubber (inner reference) and in water molecules adsorbing on each FAU, respectively. Since very small amount of silicon rubber was added into the sample tubes, the enlarged spectra at around 0ppm were also displayed in Fig. 6. Since only one signal was detected at around 5ppm, it can be considered that spin-exchange rates among the H atoms of water molecules adsorbing on each cation and those linking with other water molecules in the supercage are fast enough. Based on this result, it can be considered that whole water molecules are linked each other and we can consider only partial water molecules instead of whole ones in FAU. The CS values recorded on the ^1H MAS NMR spectra are listed in Table 2. The similar CS dependencies on cation types were obtained as those recorded on the ^{29}Si NMR spectra, i.e. large CS values were detected in Li- or Cs-type FAU. Since it is reported that the larger ^1H CS values are detected in H atoms forming the stronger H-bond [40], it can be considered that H-bonds among water molecules and the FAU frameworks are attractive in Li- and Cs-FAUs, and an origin of the complex dependencies of T_{DTG} and ^1H CS values is the same. In addition, shielding tensors of ^1H nuclei are almost determined by diamagnetic terms rather than paramagnetic components [41], therefore, it can be regarded that electron densities of H atoms in water molecules adsorbing on Li or Cs ions in the FAU framework are low. In order to reveal reasons why electron densities of water molecules are low in Li or Cs-type FAU, CS simulation was carried out.

Table 2. Chemical shift (CS) values recorded on the ^1H MAS NMR spectra. Unit is in ppm

	Si/Al Ratio				
	1.0	1.2	1.7	2.4	3.5
Cs	5.44±0.08	4.97±0.05	4.57±0.05	4.23±0.05	4.25±0.04
Rb	5.32±0.05	4.80±0.04	4.40±0.05	4.13±0.05	4.00±0.03
K	4.80±0.03	4.42±0.04	4.31±0.04	4.32±0.02	4.02±0.05
Na	4.16±0.07	4.16±0.03	4.28±0.05	4.22±0.05	4.14±0.05
Li	4.86±0.08	4.69±0.06	4.82±0.06	4.72±0.06	4.36±0.05

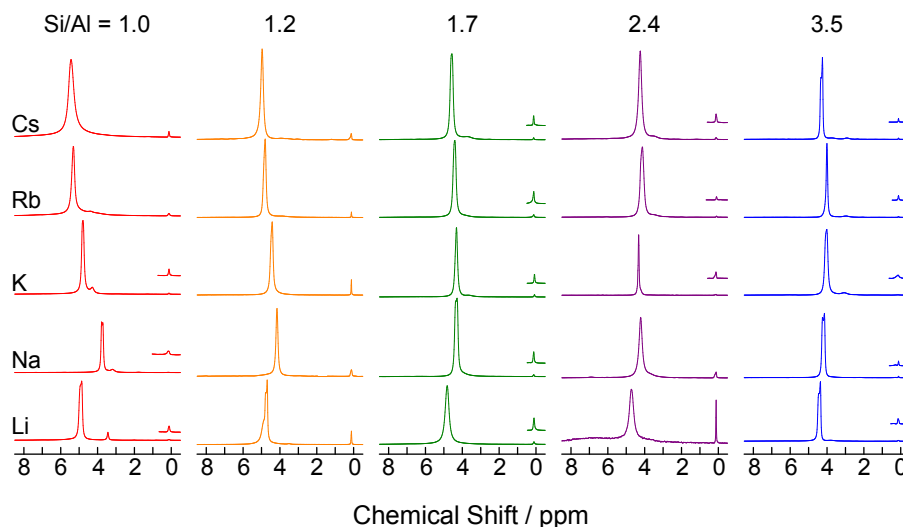


Fig. 6. ^1H MAS NMR spectra observed in M-type faujasite zeolites (M = Li, Na, K, Rb, Cs) with Si/Al ratios of 1.0, 1.2, 1.7, 2.4 and 3.5. Inner reference of silicon rubber is observed at 0.12 ppm (enlarged spectra are displayed).

3.5 Simulation

On the results of ^1H and ^{29}Si MAS NMR, and TG measurements, the lowest CS and T_{DTG} values were obtained for K- or Na-type FAUs in the same Si/Al ratio. The N_2 adsorption isotherm curves reveal that absorbable space of N_2 molecules on Rb- and Cs-type FAU is smaller than the others with the same Si/Al ratio, although the similar lattice constants among them were detected by our XRD measurements. The smaller absorbable volumes in Rb- and Cs-type FAU can be explained by the six-ring window-size of FAU frameworks: Rb^+ (296pm) and Cs^+ (338pm) have large ion-size competing with the window-size of ca. 250 pm, therefore majority parts of the ions are shared a part of supercage space as displayed in Fig. 7. In this figure, coordinates of each cation were optimized by a B3LYP/LanL2DZ function. The similar illustrations are reported for Li, K, Mg, and Ca-type zeolites [19].

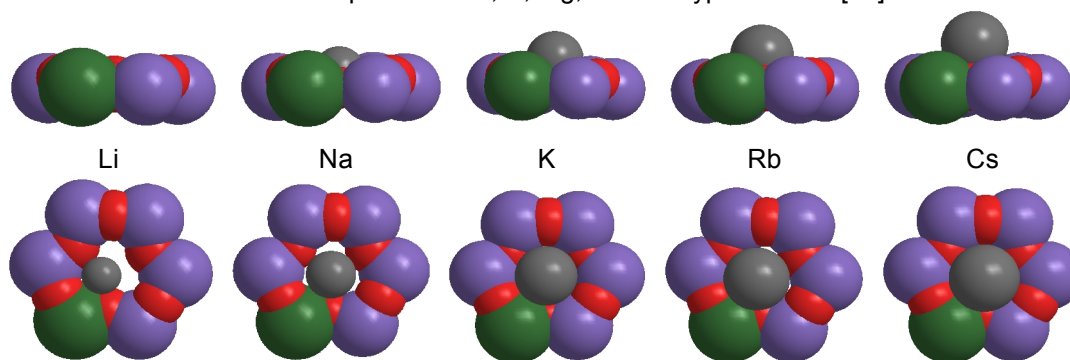


Fig. 7. Estimated locations of the cations on the six-ring windows. Si, O, Al, and cation are shown by purple, red, green, and gray, respectively

Based on this figure, we can consider a model in which number of water molecules coordinating to cations is depended on cation's size: small cations of Li^+ (120pm) and Na^+ (190pm) can insert into the FAU frameworks, therefore a few water molecules can adsorb on them, in contrast, Rb^+ and Cs^+ are located on frameworks, therefore several water molecules can link to the cations. In order to estimate coordination number of water molecules on each cation, we introduced a supercage model with chemical formula of $\text{MAiSi}_{47}\text{O}_{73}\text{H}_{48}$, ($\text{M}=\text{Li}, \text{Na}, \text{K}, \text{Rb}, \text{Cs}$). Since a reported simulation with MP2 and DFT methods in local structure models ($\text{AlSi}_7\text{O}_{14}\text{H}_{12}$, $\text{AlSi}_{10}\text{O}_{14}\text{H}_{17}$, $\text{Si}_{11}\text{O}_{24}\text{H}_{16}$, etc.) of supercage shows a good agreement with experimental values [17,20-23], our model of $\text{MAiSi}_{47}\text{O}_{73}\text{H}_{48}$ is suitable to simulate CS values. In our supercage model, reported coordinates of Si (Al) and O atoms were used and the Al atom was inserted into a part of six-ring, because experimental and theoretical reports show that whole SII is occupied by cations with a Si/Al range from 1 to 5, and occupancies of SIII and SIII' are gradually increased with decreasing Si/Al ratios in $\text{Si}/\text{Al}<2$ [9,11,42-46]. In our simulation, positions of each alkali cation, terminal H atoms of the framework, and H and O atoms in water molecules were optimized by a function of B3LYP/LanL2DZ. The coordination number of water molecules was estimated by the following process for each M-type FAU: one water molecule was initially put on the origin of this model (center of the supercage) and, then, coordinates of the water molecules and the cation and terminal H atoms were optimized. At the next step, the second water molecule was located at the origin and converged positions of two water molecules and the cation were simulated by the same function. If both water molecules can adsorb on the cation, then the same process was continued until any water molecule can't link directly to each cation. The result of coordination number of water on each cation is listed in Table 3 and illustrated in Fig. 8. This simulation showed different numbers of water molecules adsorbing on each cation.

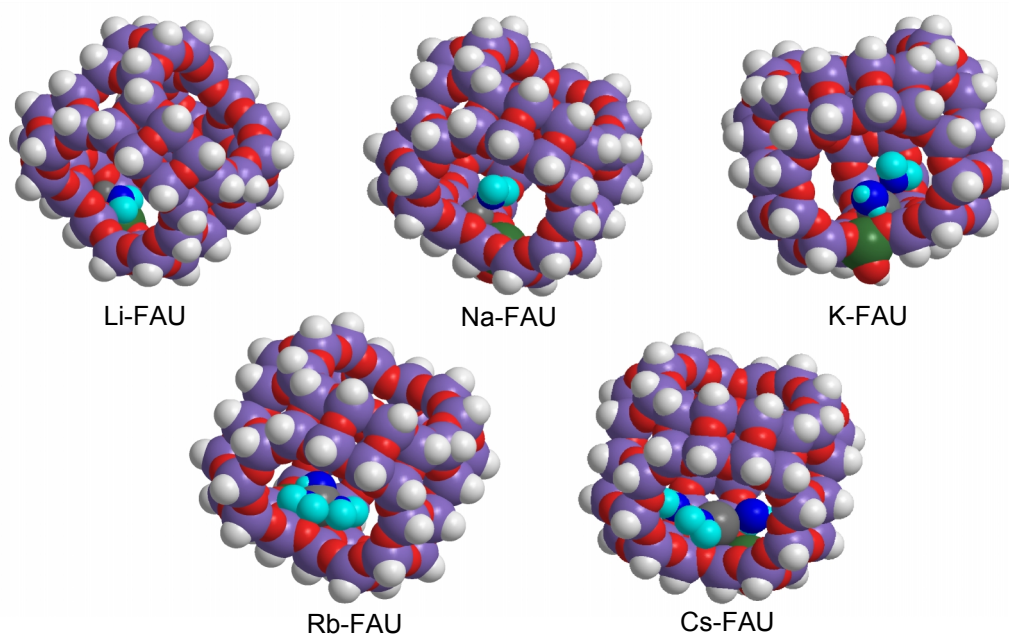


Fig. 8. Molecular arrangements of water molecules adsorbed on cations in the FAU supercage. H and O atoms of water molecules are shown by cyan and blue, respectively. Si, O, Al, H, and cation in the framework are illustrated by purple, red, green, white, and gray, respectively

Table 3. The number and ^1H chemical shift (CS) values of adsorbed water molecules on each cation in FAU estimated by MP2/cc-PVDZ function in the super cage model. Values in a case of one water molecule adsorbing on each cation are also shown

Cation	Number of water molecules	CS / ppm	
		One Water	Waters
Li	1	0.8506	0.8506
Na	2	1.0873	0.4394
K	3	1.1897	1.0634
Rb	3	1.2286	1.1346
Cs	3	1.2639	1.1482

In order to estimate CS values of water molecules, a method of ONIOM (MP2/cc-pVDZ : HF/cep-4G) was employed, where the former function of MP2/cc-pVDZ was applied for H and O atoms in water molecules and the latter was used for each cation and Si, O, Al, H atoms in the framework. The MP2/cc-pVDZ function also applied for shielding tensor estimation of a tetramethylsilan (TMS) molecule, where all coordinates of atoms were optimized by a B3LYP/6-31G** method. Subtracting shielding tensors of H atoms in the water molecules from that of TMS, ^1H CS values in the water molecules were immediately obtained as listed in Table 3. The CS values simulated in the model showed the similar tendency to those observed in ^1H MAS NMR measurements, i.e., the smallest CS value is recorded for Na-type FAU (since demonstrated ^1H CS values are rarely agreed with experimental values and CS is relative values, only tendencies are discussed in this study). Conversely, assuming another model in which only one water molecule adsorbed on each cation, CS values were monotonously increased with cation sizes, as displayed in Table 3. Therefore, it can be regarded that the difference of coordination number of water molecules influences on the complex dependences recorded on the NMR spectra. Based on our ^1H MAS NMR and TG-DTA results, it can be concluded that water molecules form weak hydrogen bonds in Na- and K-type FAU with high Si/Al ratios. In Li, Na, K Rb, and Cs ions, charge density on each surface is decreased with increasing ion radius, therefore, it can be regarded that water molecules form weaker hydrogen bonds with the larger cations. In contrast, since abundant parts of the large ions can't insert in the FAU framework, several water molecules can contact to the larger cations. Based on these two factors, the result that middle size ions of Na and K form weak hydrogen bonds with water molecules in FAU can be explained.

We also attempted to simulate the complex dependences of ^{29}Si MAS NMR CS values on cation types as displayed in Fig. 2. The supercage model was also employed in this simulation. Applying a HF/CEP-4G function to whole atoms in the model, calculated ^{29}Si CS values with respect to silanes [47] were obtained as listed in Table 4. The simulated CS values show the similar complex tendencies to those recorded on the ^{29}Si MAS NMR spectra, therefore, it can be considered that cation positions also influence on ^{29}Si CS values.

Table 4. ^{29}Si chemical shift (CS) values estimated by HF/CEP-4G function in the super cage model

Cation	CS / ppm
Li	-125.17
Na	-125.44
K	-125.63
Rb	-125.50
Cs	-125.24

4. CONCLUSION

In order to reveal adsorbed states of water molecules on faujasite-type zeolites (FAU), Na-type FAU with five different Si/Al ratio were prepared. In addition, Na ions in these five FAUs were exchanged by Li, K, Rb, or Cs ions. XRD and ^{29}Si MAS NMR spectra showed that FAU frameworks were rarely changed by ion exchanges. High-resolution solid-state ^1H MAS NMR spectra showed a signal which can be assigned to H atoms of water molecules adsorbed on each M-type FAU. Complex dependences of ^1H NMR signals on cation types were observed (the lowest CS value was recorded in Na- or K-type FAU with each Si/Al ratio). The similar tendencies were detected in TG-DTA measurements: a desorption temperature of water molecules showed complex dependences on cation properties (the minimum temperature was recorded in Na- or K-type FAU with each Si/Al ratio). In order to reveal the complex tendencies of ^1H NMR CS values, computer simulations were attempted in a supercage model. In our simulations, it was revealed that the different coordination number of water molecules to each cation results in the complex CS dependencies on cation types. The different coordination number can be accepted, because ion sizes of Li and Na ions are smaller than that of six-rings windows in the FAU framework, conversely, Rb and Cs ions are larger, i.e. abundant parts of Rb and Cs ions are occupied a part of the supercage.

COMPETING INTERESTS

Authors have declared that no competing interests exist.

REFERENCES

1. Breck DW. Zeolite molecular sieves: Structure, chemistry, and use. John Wiley: New York; 1974.
2. Rabo JA. Zeolite chemistry and catalysis. American Chemical Society: Washington; 1976.
3. Bekkum H, Flanigen EM, Jansen JC. Introduction to zeolite science and practice. Elsevier: Amsterdam; 1991.
4. Auerbach SM, Carrad KA, Dutt PK. Handbook of zeolite science and technology. Marcel Dekker: New York; 2003.
5. Yang RT. Adsorbents: Fundamentals and applications. John Wiley & Sons: New York; 2003.
6. Baerlocher C, McCusker LB, Olson DH. Atlas of zeolite framework types, 6th ed. Elsevier: New York; 2007.
7. Xu R, Pang W, Yu J, Huo Q, Chen J. Chemistry of zeolites and related porous materials: Synthesis and structure. John Wiley & Sons: Singapore; 2007.
8. Fitch AN, Jovic H, Renouprez A. Localization of benzene in sodium-Y-zeolite by powder neutron diffraction. J. Phys. Chem. 1986;90(7):1311-1318.
9. Vitale G, Mellot CF, Bull LM, Cheetham AK. Neutron diffraction and computational study of zeolite NaX: Influence of SIII' cations on its complex with benzene. J. Phys. Chem. B. 1997;101(23):4559-4564.
10. Beauvais C, Boutin A, Fuchs AH. A numerical evidence for nonframework cation redistribution upon water adsorption in faujasite zeolite. Chem. Phys. Chem. 2004;5(11):1791-1793.

11. Beauvais C, Boutin A, Fuchs AH. Adsorption of water in zeolite sodium-faujasite: A molecular simulation study. *C. R. Chim.* 2005;8(3-4):485-490.
12. Shirono K, Endo A, Daiguji H. Molecular dynamics study of hydrated faujasite-type zeolites. *J. Phys. Chem. B.* 2005;109(8):3446-3453.
13. Coasne AB, Maurin G, Henn F, Jeffroy M, Boutin A. Cation behavior in faujasite zeolites upon water adsorption: A combination of monte carlo and molecular dynamics simulations. *J. Phys. Chem. C.* 2009;113(24):10696-10705.
14. Abrioux C, Coasne B, Maurin G, Henn F, Boutin A, Lella AD, Fuchs AH. A molecular simulation study of the distribution of cation in zeolites. *Adsorption.* 2008;14(4-5):743-753.
15. Lella AD, Desbiens N, Boutin A, Demachy I, Ungerer P, Bellatc JP, Fuchs AH. Molecular simulation studies of water physisorption in zeolites. *Phys. Chem. Chem. Phys.* 2006;8:5396-5406.
16. Caillieza F, Boutinb A, Demachyb I, Fuchs AH. Thermodynamic study of water confinement in hydrophobic zeolites by Monte Carlo simulations. *Molecular Simulation.* 2009;35(1-2):24-30.
17. Limtrakul J, Treesukol P, Ebner C, Sansone R, Probst M. Structures and potential energy surface of Faujasitic zeolite/water. *Chem. Phys.* 1997;215(1):77-87.
18. Belarbi H, Haouzi A, Giuntini JC, Devautour-Vinot S, Kharroubi M, Henn F. A DFT-based model for water adsorption at aluminosilicate surfaces. Comparison with experimental data extracted from dielectric relaxation spectroscopy. *J. Non-Crystalline Solids.* 2010;356(11-17):664-668.
19. Vayssilov GN, Rosch N. Influence of alkali and alkaline Earth cations on the brønsted acidity of zeolites. *J. Phys. Chem. B.* 2001;105(19):4277-4284.
20. Bussemer B, Schroder KP, Sauer J. Ab initio predictions of zeolite structures and ^{29}Si NMR chemical shifts. *Solid State Nuc. Magn. Reson.* 1997;9(2-4):155-164.
21. Valerio G, Goursot A, Vetrivel R, Malkina O, Salahub DR. Calculation of ^{29}Si and ^{27}Al MAS NMR chemical shifts in zeolite- β using density functional theory: Correlation with lattice structure. *J. Am. Chem. Soc.* 1998;120(44):11426-11431.
22. Valerio G, Goursot A. Density functional calculations of the ^{29}Si and ^{27}Al MAS NMR spectra of the zeolite mazzite: Analysis of geometrical and electronic effects. *J. Phys. Chem. B.* 1999;103(1):51-58.
23. Ricchiardi G, Sauer J. Influence of Ti substitution on the ^{29}Si NMR spectra of silicalite. A computational study. *Z. Phys Chem.* 1999;209(1):21-32.
24. Beta IA, Bohligh H, Hunger B. Structure of adsorption complexes of water in zeolites of different types studied by infrared spectroscopy and inelastic neutron scattering. *Phys. Chem. Chem. Phys.* 2004;6:1975-1981.
25. Kathoh M, Koide R, Yamada K, Yoshida T, Horikawa T. IR Spectroscopic analysis of thermal behavior of adsorbed water on Y-type zeolite. *International J. Mod. Phys.* 2012;6:437-442.
26. Ferwerda R, Maas JH. The influence of adsorbed molecules on the framework vibrations of Na-FAUJASITES studied with FT Raman spectroscopy. *Spectrochimica Acta A.* 1995;51(12):2147-2159.

27. Duer MJ. Solid-State NMR Spectroscopy: Principles and applications. Blackwell Science: Tokyo; 2002.
28. Fitzgerald JJ. Solid-state NMR spectroscopy of inorganic materials. American Chemical Society: Washington; 1999.
29. Semmer-Herle'dan V, Heeribout L, Batamack P, Dore'mieux-Morin C, Fraissard J, Gola A, Benazzi E. Comparison of the acid strength of dealuminated H-faujasites determined by ^1H NMR after water adsorption. *Microporous Mesoporous Mater.* 2000;34(2):157-169.
30. Freude D, Hunger M, Pfeifer H. Study of brønsted acidity of zeolites using high-resolution proton magnetic resonance with magic-angle spinning. *Chem. Phys. Lett.* 1982;91(4):307-310.
31. Freude D, Hunger M, Pfeifer H, Schwieger W. ^1H MAS NMR studies on the acidity of zeolites. *Chem. Phys. Lett.* 1986;128(1):62-66.
32. Freude D, Kilinowski J, Hamdan H. Solid-state NMR studies of the geometry of brønsted acid sites in zeolitic catalysts. *Chem. Phys. Lett.* 1988;149(4):355-362.
33. Jelinek R, Ozkar S, Pastore H, Malek A, Ozin GA. Guest-host interactions in sodium zeolite Y: Structural and dynamical ^{23}Na double-rotation NMR study of water, trimethylphosphine, molybdenum hexacarbonyl, and $\text{Mo}(\text{CO})_4(\text{PMe}_3)_2$ adsorption in Na56Y. *J. Am. Chem. Soc.* 1993;115(2):563-568.
34. Legras B, Polaert I, Estel L, Thomas M. Mechanisms responsible for dielectric properties of various faujasites and linde type A zeolites in the microwave frequency range. *J. Phys. Chem. C.* 2011;115(7):3090-3098.
35. Iwai Y, Oka N, Yamanishi T. Influence of framework silica-to-alumina ratio on the water adsorption and desorption characteristics of MHI-CaX/CaY zeolite. *J. Phys. Chem. Solids.* 2009;70(5):881-888.
36. Yang H, Ping Z, Niu G, Jiang H, Long Y. TG/DTG/DTA Study on Interaction between the framework of high silica hydrophobic FAU zeolite and adsorbed organics. *Langmuir.* 1999;15(16):5382-5388.
37. Robson H. *Verified syntheses of zeolite materials* : Elsevier Science Ltd.; 2001.
38. Yang S, Navrotsky A. Energetics of formation and hydration of ion-exchanged zeolite Y. *Microporous Mesoporous Mater.* 2000;37(1-2):175-186.
39. Lia YQ. Crystal radii and effective ionic radii of the rare earth ions. *J. Solid State Chem.* 1991;95(1):184-187.
40. Honda H. ^1H -MAS-NMR chemical shifts in hydrogen-bonded complexes of chlorophenols (Pentachlorophenol, 2,4,6-Trichlorophenol, 2,6-Dichlorophenol, 3,5-Dichlorophenol, and *p*-Chlorophenol) and amine, and H/D isotope effects on ^1H -MAS-NMR spectra. *Molecules.* 2013;18(4):4786-4802.
41. Gerstein BC, Dybowski CR. *Transient techniques in NMR of solids.* Academic Press: New York; 1985.
42. Eulenberger GR, Shoemaker DP, Keil JG. Crystal structures of hydrated and dehydrated synthetic zeolites with faujasite aluminosilicate frameworks. I. The dehydrated sodium, potassium, and silver forms. *J. Phys. Chem.* 1967;71(6):1812-1819.

43. Jiráček Z, Vratislav S, Bosáček V. A neutron diffraction study of H, Na-Y zeolites. *J. Phys. Chem. Solids*. 1980;41(10):1089-1095.
44. Olson DH. The crystal structure of dehydrated NaX. *Zeolites*. 1995;15(5):439-443.
45. Zhu L, Seff K. Reinvestigation of the crystal structure of dehydrated sodium zeolite X. *J. Phys. Chem. B*. 1999;103(44):9512-9518.
46. Porcher F, Souhassou M, Dusausoy Y, Lecomte C. The crystal structure of a low-silica dehydrated NaX zeolite. *Eur. J. Miner.* 1999;11(2):333-343.
47. Heine T, Goursot A, Seifert G, Weber J. Performance of DFT for ^{29}Si NMR chemical shifts of SILANES. *J. Phys. Chem. A*. 2001;105(3):620-626.

© 2014 Morita et al.; This is an Open Access article distributed under the terms of the Creative Commons Attribution License (<http://creativecommons.org/licenses/by/3.0>), which permits unrestricted use, distribution, and reproduction in any medium, provided the original work is properly cited.

Peer-review history:

The peer review history for this paper can be accessed here:
<http://www.sciencedomain.org/review-history.php?iid=536&id=7&aid=5011>